Los Alamos National Laboratory is operated by the University of California for the United States Department of Energy under contract W-7405-ENG-36

CONF-8505150--1

LA-UR--85-1728

DE85 012730

TITLE THE KIVA COMPUTER PROGRAM FOR MULTIDIMENSIONAL CHEMICALLY REACTIVE FLUID FLOWS WITH FUEL SPRAYS

AUTHOR(S) Peter J. O'Rourke

SUBMITTED TO Symposium on Numerical Simulation of Combustion Phenomena, May 21-24, 1985, Sophia-Antipolis, France

DISCLAIMER

Los Alamos Los Alamos National Laboratory
Los Alamos, New Mexico 87545

THE KIVA COMPUTER PROGRAM FOR MULTIDIMENSIONAL CHEMICALLY REACTIVE FLUID FLOWS WITH FUEL SPRAYS

Peter J. O'Rourke
Group T-3
Los Alamos National Laboratory
Los Alamos, New Mexico 87454 USA

I. INTRODUCTION

This paper is a presentation of the capabilities of the KIVA computer program,[1,2] which was written to calculate both two- and three-dimensional chemically reactive fluid flows. KIVA solves by finite-difference techniques the unsteady equations for a multi-component, chemically reactive mixture of ideal gases, together with those for an evaporating liquid spray. Although it was written with applications to internal combustion engine research in mind, with modification KIVA can be applied to a variety of other combustion and two-phase flow problems. This paper emphasizes the differences between KIVA and the well-known CONCHAS-SPRAY computer program[3] and gives some advantages and disadvantages of the numerical methodology in KIVA. We illustrate the capabilities of the program by describing the results of numerical test problems.

Like CONCHAS-SPRAY, KIVA utilizes the ALE (Arbitrary Lagrangian-Eulerian) method.[4] The advantages of the ALE method are its geometric flexibility and the fact that the finite difference approximations can be easily formulated to conserve momentum. A disadvantage of the ALE method is its susceptibility to alternate node uncoupling.[1,3] This problem is more pronounced in KIVA than in CONCHAS-SPRAY, and in the first section of this paper we tell why this is so and indicate some ways that are being considered to overcome the problem.

KIVA, like CONCHAS-SPRAY, possesses an arbitrary Mach number capability--that is, the same computer program can be used to calculate both subsonic and supersonic flows. This capability is implemented differently, however, in KIVA. Instead of the implicit ICE method[5] used in CONCHAS-SPRAY, KIVA uses an acoustic subcycling method[6] coupled with methods for scaling the Mach number[7] and for damping high frequency acoustic waves.[8] The acoustic subcycling algorithm is described in section two of this paper.

Section three describes two changes to the particle method[9] for calculating liquid sprays. First, KIVA includes a calculation of drop collisions and coalescence,[10] which influence significantly the dynamics of many Diesel and stratified charge engine sprays. Second, KIVA

radii at injection. With the new sampling method, fewer particles are needed to obtain results that are independent of number of particles.

We mention here three additional improvements in KIVA. The subgrid scale turbulence model used in CONCHAS-SPRAY has been generalized by the inclusion of a transport equation for subgrid scale turbulent kinetic energy. Second, KIVA has an improved method for calculating chemical equilibria.[11] Third, KIVA has been written for the CRAY computer and makes extensive use of the vector calculation feature of this computer. Partly for this reason, KIVA can perform many two-dimensional calculations more than five times faster than CONCHAS-SPRAY.

II. THE ALE METHOD

In the ALE method, spatial differences are formed with respect to a mesh of arbitrary quadrilateral cells in two dimensions and hexahedral cells in three dimensions. As is shown in Fig. 1, the positions and velocities of cell vertices are stored in computer memory. All thermodynamic variables are located at cell centers. The computational cycle is divided into three phases (cf. Fig. 4). In phase A the chemical source terms and heat and mass diffusion terms are calculated. In phase B, we calculate the pressure gradient accelerations and changes to the density and internal energy due to divergence of the velocity field. This is accomplished by the acoustic subcycling algorithm in

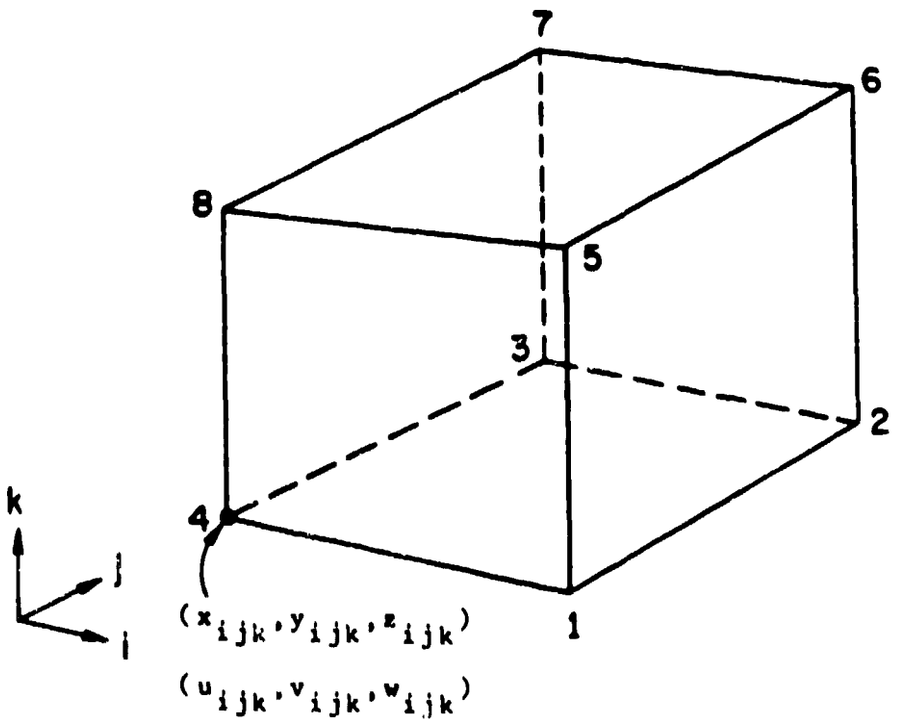

Fig. 1. Typical Finite-difference cell.

KIVA. In phases A and B, the computational mesh is moved in a purely Lagrangian fashion. In phase C the mesh is remapped or rezoned into another mesh, and the resulting convection is calculated. One appealing feature of the ALE method is that the mesh can be moved in a fairly arbitrary fashion.

A disadvantage of the ALE method, the alternate node uncoupling problem, arises because of the above cell variable locations. As has been previously shown,[12] when the ALE method is applied to the acoustic wave equations on a two-dimensional square mesh, the resulting finite difference approximation to the Laplacian operator is skewed; that is

$$FD(\nabla^2 P)_{i,j} = \frac{1}{2\delta x^2}\left(P_{i+1,j+1} + P_{i+1,j-1} + P_{i-1,j+1} + P_{i-1,j-1} - 4P_{i,j}\right) \tag{1}$$

where FD( ) denotes the finite difference approximation to the quantity in parentheses. It is seen that the sum of the subscripts in each pressure term in (1) differs from i+j by an even integer. As a result, pressure disturbances will propagate in a "checkerboard" fashion; an acoustic disturbance in a red checkerboard square or cell, will propagate to red cells but not to black cells. This phenomenon is clearly shown in Fig. 2, where plots are given of the computer-generated pressure fields and velocity vectors from a KIVA calculation of the propagation of a small pressure disturbance. Initial conditions were a quiescent, uniform fluid except in one cell where the pressure was slightly elevated. The velocity vectors in Fig. 2 show the characteristic "hourglass" mode that is often seen in ALE-method calculations.

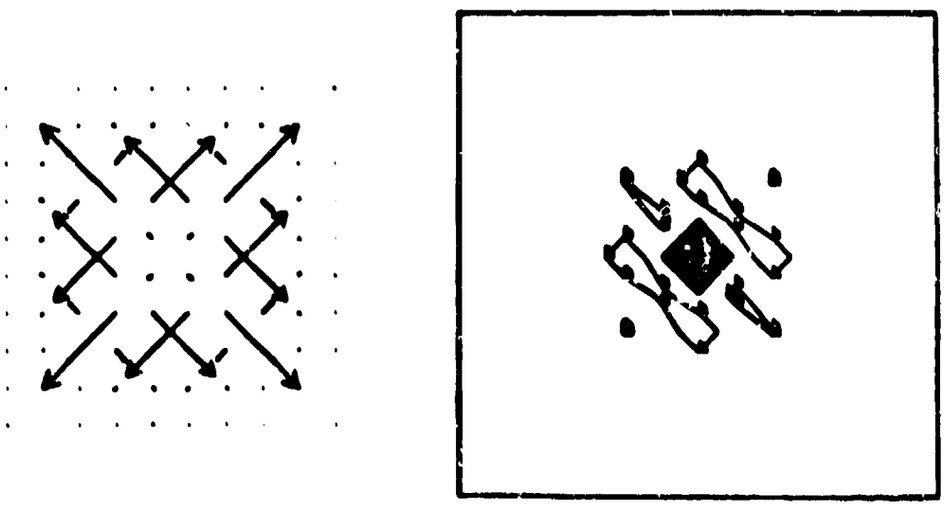

Fig. 2. Velocity vectors and pressure contours showing alternate node uncoupling.

Alternate node uncoupling is often seen in KIVA calculations in which there are strongly exothermic chemical reactions. The reason is that chemical reaction rates often have very sensitive temperature dependencies. Small temperature differences give rise to large differences in reaction rate. Thus if in one computational cell the temperature is slightly elevated above that in neighboring cells, the elevated local heat release rate gives rise to a pressure disturbance that will generate numerical pressure and velocity oscillations, just as in the example of Fig. 2.

Figure 3 gives an example of this phenomenon from an internal combustion engine calculation. Shown are velocity vectors and contours of pressure, temperature, and fuel mass fraction. The temperature and fuel mass fraction plots show well-behaved temperature and fuel mass fraction variations, with steepest gradients occurring in a region of strong premixed combustion. Precisely in this region is where the velocity vectors and pressure contours show oscillations characteristic of alternate node uncoupling.

The above mechanism for alternate node uncoupling is present in both CONCHAS-SPRAY and KIVA, but its effects are more pronounced in KIVA because the fully-implicit ICE formulation in CONCHAS-SPRAY numerically damps the acoustic mode much more than the subcycling algorithm in KIVA.[13] Smaller acoustic wave pressure gradients and velocities im-

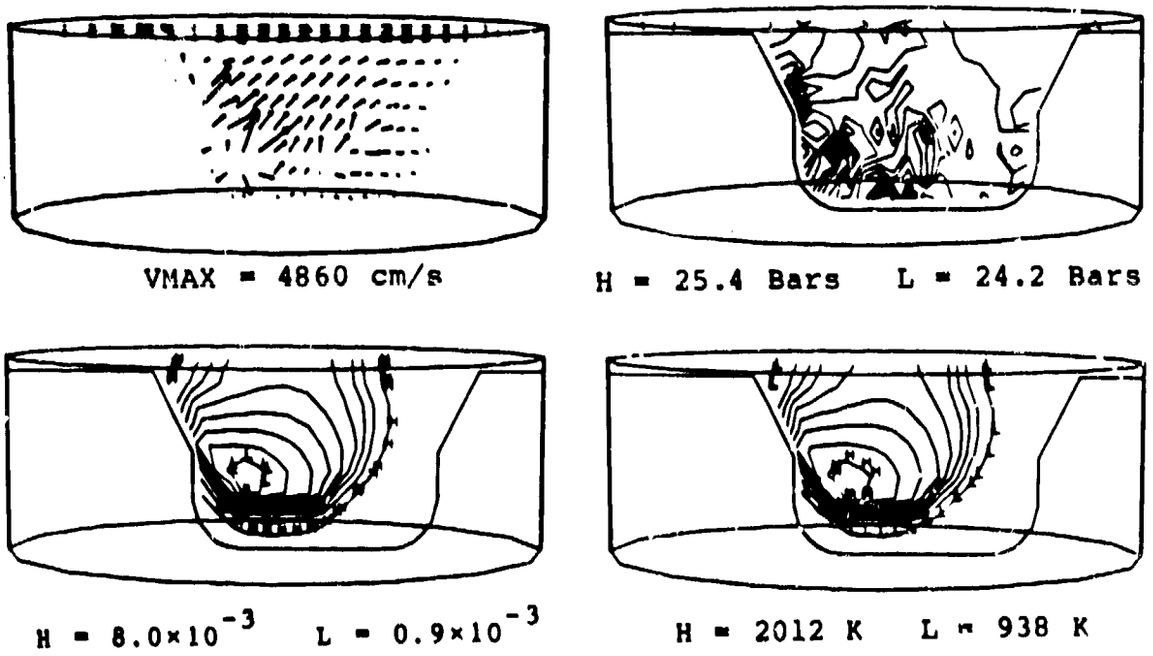

Fig. 3. Plots of velocity vectors and contours of pressure (upper right), fuel mass fraction (lower left), and temperature (lower right) from a KIVA engine calculation.

ply that less alternate node uncoupling will be produced. This suggests one means to reduce the alternate node uncoupling problem in KIVA-use of the fully-implicit ICE formulation. The fundamental problem - that the acoustic mode cannot be calculated accurately by the ALE method - is thereby bypassed by strongly damping acoustic waves. In most combustion applications this is not a problem because acoustic wave effects are unimportant.

To cure the fundamental problem, however, a method must be devised to couple the solutions in the red and black "checkerboard" cells. One remedy is to locate velocities on cell faces during all or part of the computational cycle. Methods that locate velocities on cell faces, do not suffer from alternate node uncoupling.[14,15] A difficulty with methods of this type, however, is that their geometric flexibility is usually reduced; for example, computational meshes are often required to be orthogonal.[15] This remedy and others are currently under investigation.

III. THE ARBITARY MACH NUMBER CAPABILITY

The KIVA program can be used to calculate flows at arbitrary Mach number. An acoustic subcycling algorithm[6] is currently utilized to overcome the computational inefficiency that besets many compressible flow computer programs when applied to low Mach number problems. The general idea of acoustic subcycling is illustrated in Fig. 4. Those terms associated with pressure wave progagation are differenced in phase B with a time step δt_s that can in general be a submultiple of the main computational time step δt. Phase B uses an explicit method that requires that the Courant condition $\frac{c\delta t_s}{\delta x} \lesssim 1$ be satisfied.[13] Here c is the speed of sound and δx is the computational cell size. The remaining terms in the equations are differenced with time step δt that is governed by the constraint $\frac{u\delta t}{\delta x} \lesssim 1$, where u is the fluid velocity. If $\frac{u\delta t}{\delta x} \approx 1$ and $\frac{c\delta t_s}{\delta x} \approx 1$, as is often true, then

$$\frac{\delta t}{\delta t_s} \approx \frac{c}{u} \approx 1/M \quad , \tag{2}$$

and $\delta t_s \ll \delta t$ when $M \ll 1$. Computational efficiency is gained in low Mach number problems because only a small number of terms are differenced using δt_s, while the remaining terms, whose values vary slowly on the time scale of acoustic wave propagation, are differenced using δt.

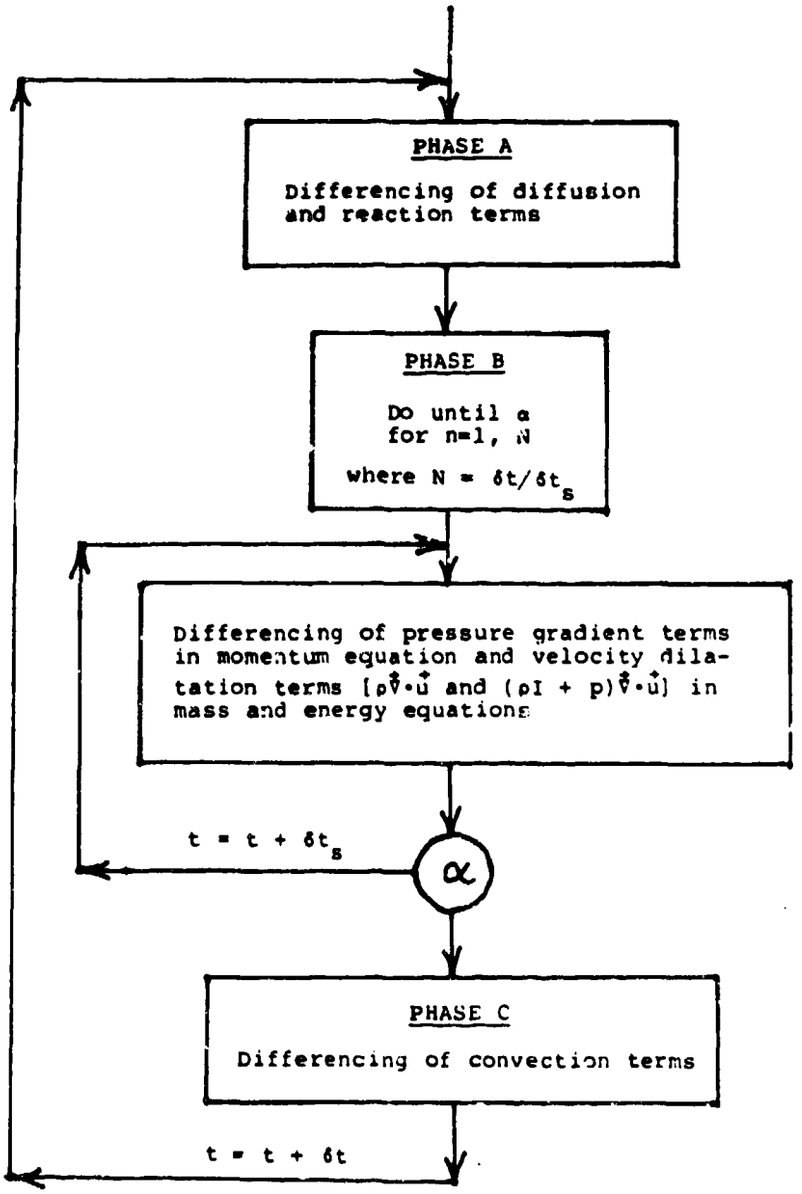

Fig. 4. Simplified flow chart of KIVA computational cycle.

An advantage of acoustic subcycling over the ICE method is that the acoustic mode is calculated more accurately. The finite difference approximations of the acoustic subcycling method are neutrally stable as long as $\frac{c\delta t_s}{\delta x} \leq 1$. This means that there is no numerical damping of computed acoustic waves.[13] In contrast, acoustic waves are strongly damped by the ICE method, even when $\frac{c\delta t}{\delta x} \approx 1$.[13] This is illustrated in Fig. 5 where we compare Riemann problem solutions obtained with KIVA and with CONCHAS-SPRAY, which uses the ICE method. The implicit damping in the CONCHAS-SPRAY calculation is especially evident at the head and foot of the rarefaction region.

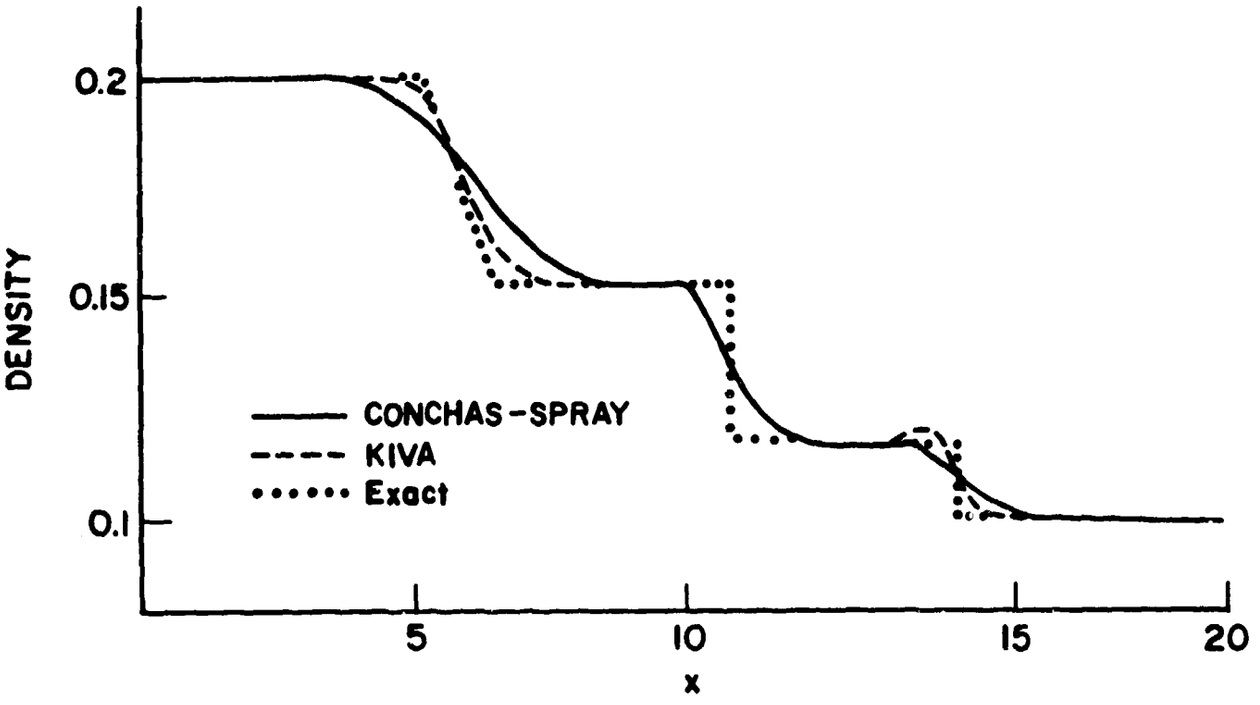

Fig. 5. Riemann problem solutions.

We have modified the acoustic subcycling method to eliminate two of its disadvantages. First, according to Eq. (2), the number of subcycles per computational cycle is approximately 1/M. Thus, when the Mach number is very small, the method is inefficient. To remedy this, we use acoustic subcycling in conjunction with the Pressure Gradient Scaling method.[7] This is a technique for increasing the Mach number M to a larger value, while keeping fixed all the other dimensionless variables that characterize the physical problem of interest. In practice, we find that in very low Mach number problems, we can increase M to 0.1 without significantly altering solution features of interest.

The second disadvantage of acoustic subcycling is that even short wavelength (L/δx small) acoustic waves are undamped numerically. These waves are not resolved; for example, there is still considerable numerical dispersion associated with acoustic subcycling.[13]

To remedy this, we have added to the momentum equation an explicit damping term of the form

$$\vec{\nabla}\left\{a\rho c^2 \delta t_s [\vec{\nabla}\cdot\vec{u} - (\vec{\nabla}\cdot\vec{u})_o]\right\} \quad , \tag{3}$$

where 'a' is a constant usually taken to be unity, ρ is the mixture density, and $(\vec{\nabla}\cdot\vec{u})_o$ is the elliptic divergence of the velocity field.[8]

The elliptic divergence is the value $\vec{\nabla}\cdot\vec{u}$ would have if the pressure field were uniform in space - that is, in the absence of acoustic waves. If $(\vec{\nabla}\cdot\vec{u})_o = 0$, then (3) would have the form of a rate of momentum change due to a bulk viscosity. In a calculation in which the acoustic waves are very small, $\vec{\nabla}\cdot\vec{u} \approx (\vec{\nabla}\cdot\vec{u})_o$ and (3) would have no effect. In the absence of damping mechanisms other than (3), the damping time of a wave of length L will be approximately $L^2/(ac^2\delta t_s)$, and thus short wavelength components will be most quickly damped. For more details concerning the implementation of (3) the reader is referred to Ref. [8].

Even with the above numerical damping, unphysical and very long-lived acoustic waves can be introduced in calculations. Often this arises due to discontinuities that are present in one's initial conditions. An example is given in Fig. 6, which displays results from two KIVA calculations of the compression of an unreacting gas in an engine cylinder. The oscillatory solution is obtained when the piston is begun impulsively from its position at a crank angle of 90° BTDC (before

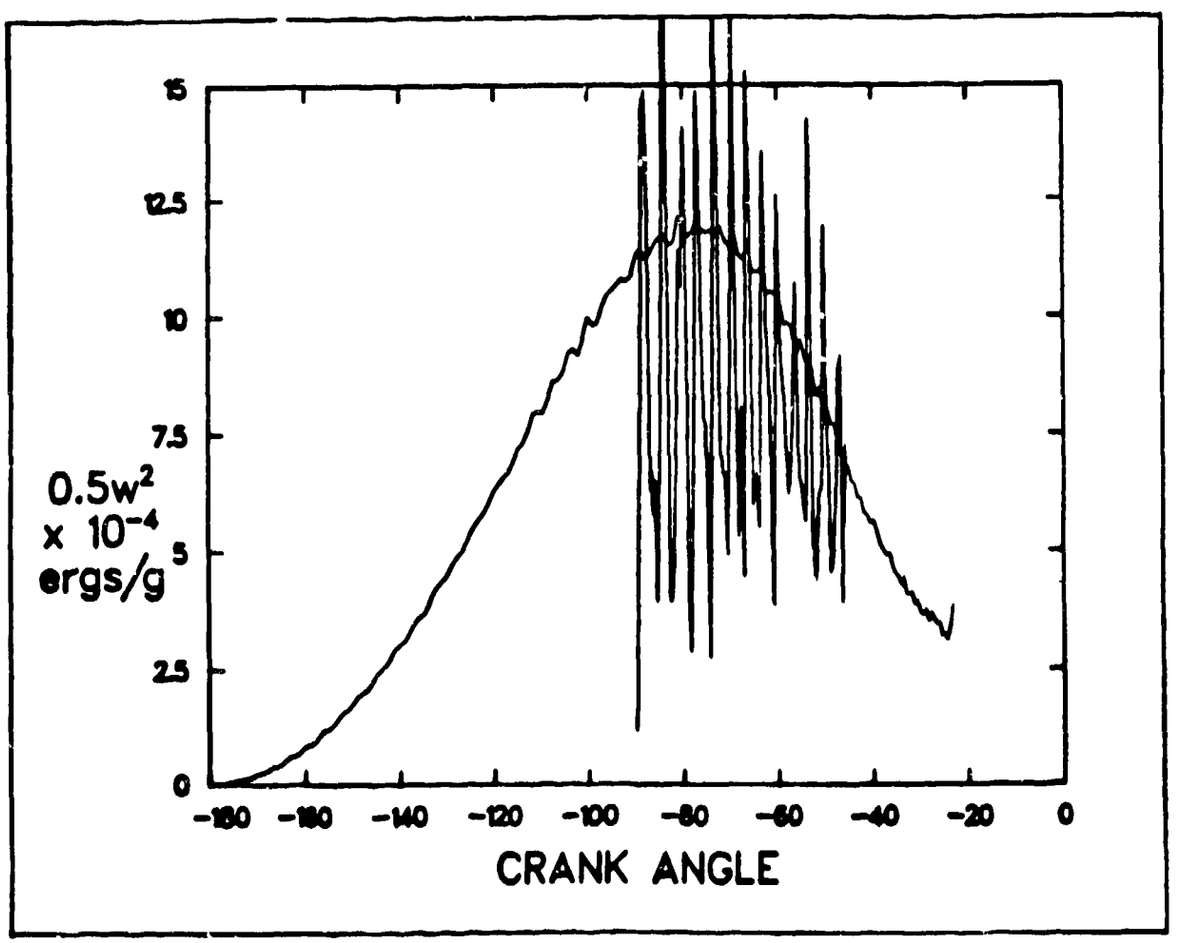

Fig. 6. Specific axial kinetic energy versus time from calculations

top-dead-center), and the smooth solution is obtained when the piston is begun at zero velocity from its position at 180° BTDC.

Finally, the user of KIVA is cautioned that in order to calculate accurately the interaction of acoustic waves with chemical or diffusive processes, it is still necessary to calculate with $c\delta t/L < 1$, where L is the wavelength of those waves of interest and δt is the main computational time step. This criterion says that an acoustic wave can travel only a fraction of its wavelength in one time step, and allows chemical or diffusive terms to respond to changes in the fluid variables due to passage of the acoustic waves. Since $\frac{c\delta t_s}{\delta x} \approx 1$ in low speed combustion problems, resolved acoustic waves must have wavelengths L such that

$$L > c\delta t \approx c\,\frac{\delta t_s}{M} = \frac{dx}{M} \quad , \tag{4}$$

where we have used Eq. (2). Thus when M = 0.1, we are at best resolving wavelengths greater than $10\delta x$. This is yet another reason for the numerical damping supplied by (3). In order to resolve smaller wavelengths, one needs to legislate a smaller time step δt than that given by the condition $\frac{u\delta t}{\delta x} \approx 1$.

IV. SPRAY MODEL IMPROVEMENTS

The dynamics of liquid fuel sprays are calculated in KIVA using the stochastic particle method.[9] In this method, the spray is represented by computational particles. Each particle represents a number of drops with identical size, velocity, and temperature. By "stochastic", we mean that we sample randomly from distributions assumed to govern drop properties when they are formed near the injector and drop behavior at downstream locations.

KIVA contains two improvements to the stochastic particle method as implemented in CONCHAS-SPRAY. First, we have incorporated a calculation of drop collisions and coalescences in KIVA. Second, KIVA uses a more efficient method for sampling from the distribution of drop radii at formation.

A. The Drop Collision Model

In this section we discuss briefly some assumptions concerning the dynamics of drop collisions and the manner in which these collisions are calculated. For more details, the reader is referred to [1], [10],

and [16]. A fundamental assumption of the spray model in KIVA is that the liquid droplets occupy a negligible volume fraction ϵ of the two-phase, gas-liquid mixture; that is, $\epsilon \ll 1$. When this condition is violated, a number of complicated thick spray effects[16] became important, and these effects are not accounted for by the model. Concerning drop collisions, the assumption that $\epsilon \ll 1$ allows us to consider only binary collisions and treat these as instantaneous events. Thus we can use a collision integral similar to that used in the Bolzmann equation for dilute gases.[17] We now show why this is so. As in the kinetic theory of gases the drop-drop interaction frequency ν_{int} can be roughly estimated to be the product of the average relative velocity between drops v_{rel}, the number density of drops n_o, and the cross section for interaction. If the interaction cross section is approximately the droplet cross-sectional area A, the formula for ν_{int} is

$$\nu_{int} \approx n_o v_{rel} A \quad .$$

Letting ϵ denote the volume fraction occupied by the drops and d a characteristic drop diameter, since $\epsilon \approx n_o A d$, we have

$$\nu_{int} \approx \epsilon \frac{v_{rel}}{d} \quad .$$

v_{rel}/d is approximately the time spent in collisions t_{coll}. We obtain for the time between interactions t_{int},

$$t_{int} = 1/\nu_{int} \approx \frac{t_{coll}}{\epsilon} \quad . \tag{5}$$

Thus if $\epsilon \ll 1$, the time spent in collisions is a small fraction of the time between collisions.

A number of other assumptions are made concerning drop collision dynamics. First, it is assumed that the collision cross section is equal to the geometric cross section. While this is a poor assumption for some applications,[18] there are arguments that it is a good assumption for engine sprays.[16] Second, it is assumed that there are two outcomes of a collision: coalescence or grazing collision. These are illustrated in Fig. 7. In a grazing collision, the drops temporarily coalesce, but then separate again because their relative velocity is large. Experiments[19] show that small satellite drops are often pro-

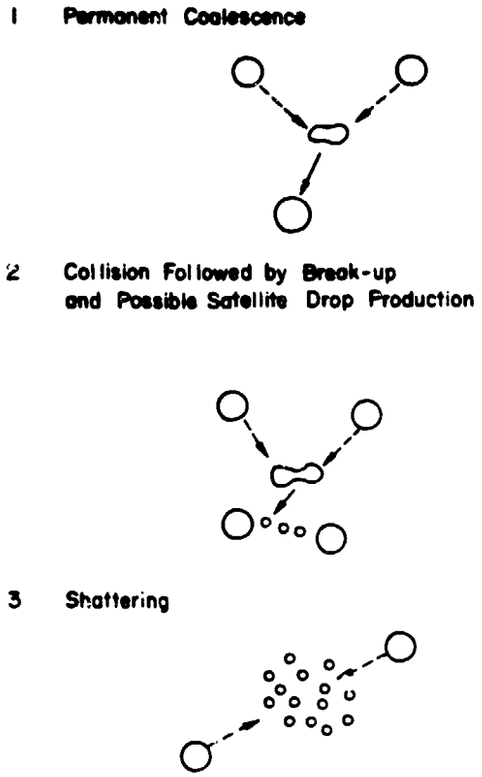

Fig. 7. Possible results of a binary drop collision.

duced by grazing collisions. In our model, satellite drop production is ignored. We also ignore the third type of collision illustrated in Fig. 7, shattering collisions, which occur at very large relative velocities. Despite the uncertainties in some of these assumptions, this model has had impressive successes in predicting the evolution of drop sizes in experimental sprays.[20, 21]

We now describe briefly the basic idea of our collision calculation. Consistent with the viewpoint of the stochastic particle method,[16] drop collisions are calculated by a sampling procedure. The alternative is to try to represent the complete distribution of drop properties that arise due to drop collisions. For example, having calculated the collision frequency between a drop associated with particle A and all drops associated with another particle, we could proceed in two ways. In the first way, we could use the collision frequency to calculate the probable number of drops in particle A that undergo collisions with drops in the other particle. To represent the distribution of collision behavior, this number of drops would be subtracted from particle A, and one or more new particles would be created having the properties of the drops resulting from the collisions. We tried such a procedure with the result that we quickly had more particles than could be accommodated by computer storage. In the second way,

which is the way we use, the collision frequency is used to calculate the probability P that a drop in particle A will undergo a collision with a drop in the other particle. Then all the drops in particle A behave in the same manner; they either do or do not collide, and the probability of the former event is P. Since all the drops in particle A behave in the same way, no new particles have to be created. Then the probability distribution of outcomes is recovered by ensemble averaging over many computations, or, in a steady-state calculation, by time averaging over a long time.

B. Improved Sampling Procedure

We have implemented in KIVA a more efficient method for sampling from the distribution of drop radii of newly formed drops. It is more efficient in the sense that fewer computational particles are needed to obtain results that are independent of particle numbers. We assume a distribution f(r), where f(r)dr is the probability that a new drop's radius lies in the interval (r, r+dr). In KIVA, $f(r) = 1/\bar{r} \exp(-r/\bar{r})$, where $\bar{r}$ is the number-averaged drop radius. The precise form of f(r) is irrelevant, however, for the present discussion. Also associated with the sampling procedure is a second distribution g(r), where g(r)dr is the probability that the radius associated with a new computational particle lies in the interval (r, r+dr). Thus f(r)/g(r) equals the number of drops per computational particle. In CONCHAS-SPRAY, g(r) is a uniform distribution in the interval (r_{min}, r_{max}), where $r_{min} \ll \bar{r}$ and $r_{max} \gg \bar{r}$. We have found that it is more efficient to sample most frequently those drop radii where the most mass is located. The reason is that usually these drops exert the most influence on the gas through exchange of mass, momentum, and energy. Since the mass distribution of newly formed drops is proportional to $r^3 f(r)$, we take $g(r) \sim r^3 f(r)$. This idea was first used in Ref. [16].

C. KIVA Calculations of Spray Combustion

Direct combustion of sprays is important in a number of combustion devices but is poorly understood partly because of the complexity of solving equations of motion for two-phase, chemically reacting flows. In this section we present some preliminary results of KIVA calculations of spray combustion. The experimental kerosene spray, shown schematically in Fig. 8, issues from an axisymmetric hollow cone injector, and a swirling air flow is introduced through a coaxial duct at the level of the spray injector. A highly turbulent and sooting diffusion flame is observed above the injector. If the swirl velocity of

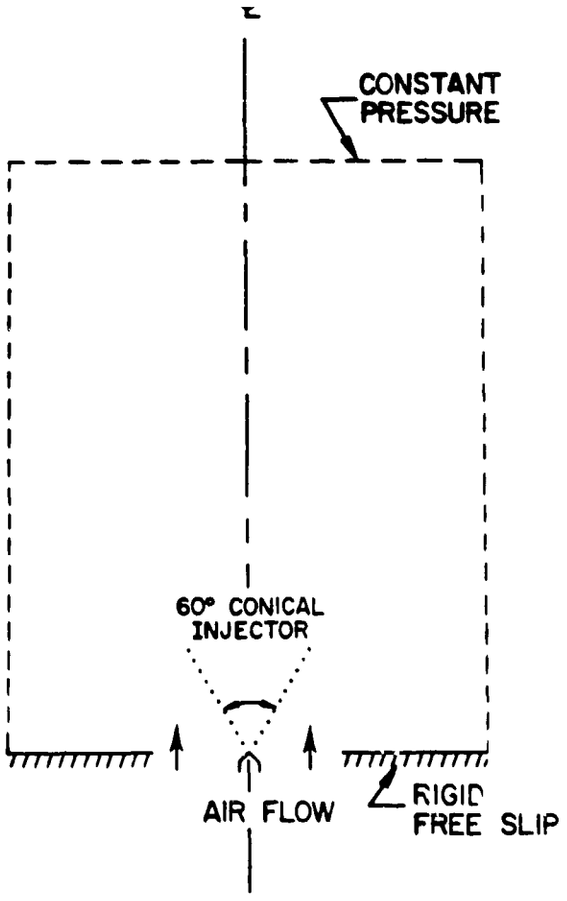

Fig. 8. Schematic drawing of spray combustor.

the air is large enough, the flame is observed to lower toward the plane of the inlet air duct.

Figure 9 gives plots from a KIVA calculation of this flame. Shown are velocity vectors and spray particle positions as well as temperature, equivalence ratio, and droplet Sauter mean radius contours. These show three stages in the formation and combustion of the fuel/air mixture. Near the injector, there is an entrainment region where air is drawn into the spray. The entrained air flow draws the smaller drops into the interior of the spray cone. Because of the cool temperatures there, little vaporization occurs and the gas mixture is fuel lean. A region of premixed combustion is observed above the entrainment region. Most of the spray droplets are vaporized here, and most of the oxygen in the core of the spray is consumed. Above the premixed flame region is the region of diffusion flame burning. The equivalence ratio contours here separate fuel-rich and fuel-lean zones and indicate the diffusion flame position.

One question that arises concerning such flames is what determines the height of the premixed flame above the injector. Preliminary re-

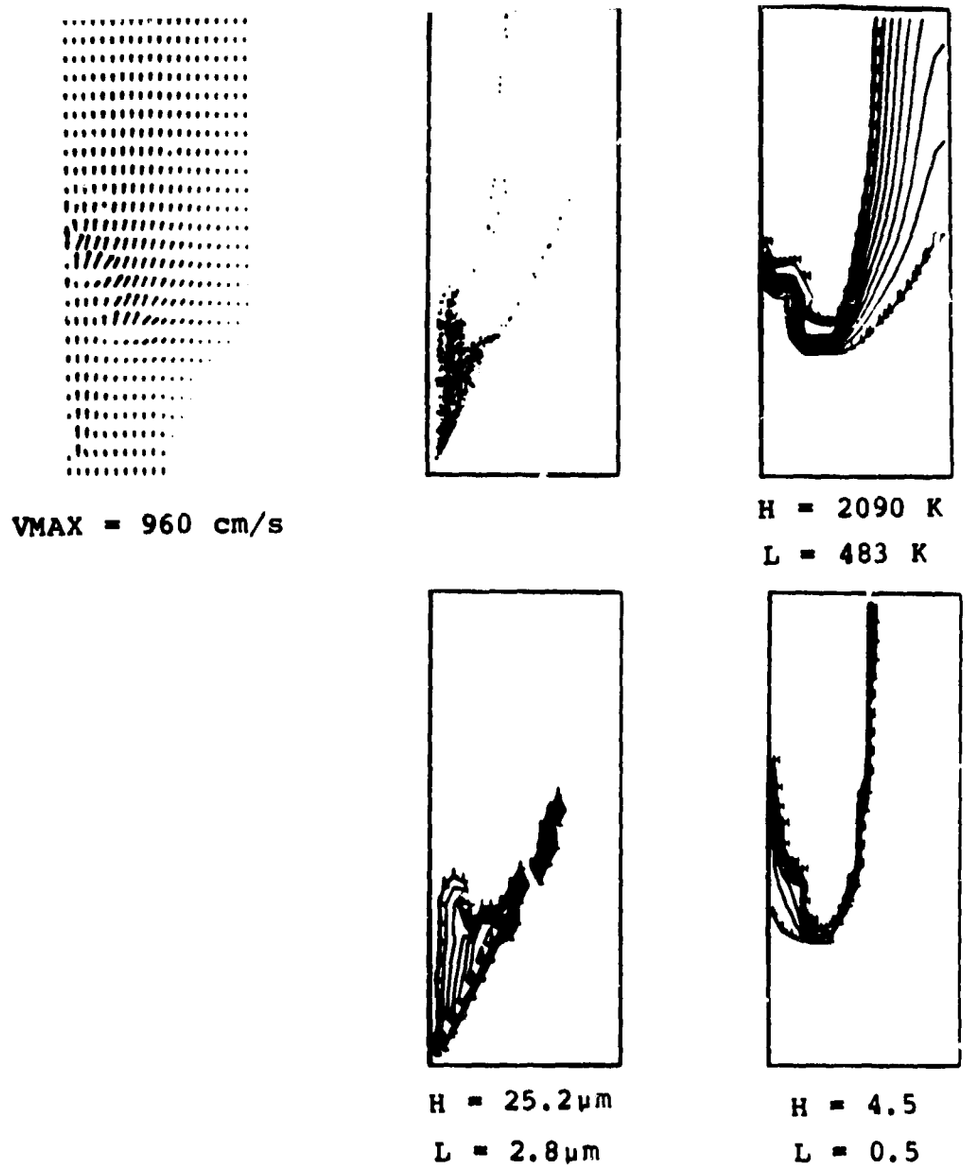

Fig. 9. Plots of velocity vectors, spray particle positions, and contours of temperature (upper right), droplet Sauter mean radius (lower left), and equivalence ratio (lower right) from spray combustion calculation.

sults show a dependence of steady flame position on ignition location and a strong dependence on the assumed droplet sizes near the injector. Another possible factor not presently included in the model, is heat loss to the upstream boundary. The KIVA program is currently being used to systematically explore these physical influences and thus give a more detailed understanding of spray combustion.

ACKNOWLEDGMENTS

The author would like to thank T. D. Butler, A. A. Amsden, J. D. Ramshaw, and L. D. Cloutman for help in the preparation of this manuscript.

REFERENCES

1. A. A. Amsden, et al., "KIVA: A Computer Program for Two- and Three-Dimensional Fluid Flows with Chemical Reactions and Fuel Sprays," Los Alamos National Laboratory report LA-10245-MS (1985).

2. A. A. Amsden, et al., "KIVA: A Comprehensive Model for 2D and 3D Engine Simulations," SAE paper 850554 (1985).

3. L. D. Cloutman, et al. "CONCHAS-SPRAY: A Computer code for Reactive Flows with Fuel Sprays," Los Alamos National Laboratory Report LA-9294-MS (1982).

4. C. W. Hirt, et al., J. Comput. Phys. 14, 227 (1974).

5. F. H. Harlow and A. A. Amsden, J. Comput. Phys. 8, 197 (1971).

6. L. C. Haselman, "TDC--A Computer Code for Calculating Chemically Reacting Hydrodynamic Flows in Two Dimensions," Lawrence Livermore Laboratory report UCRL-52931 (1980).

7. J. D. Ramshaw, P. J. O'Rourke, and L. F. Stein, "Pressure Gradient Scaling Method for Fluid Flow with Nearly Uniform Pressure," J. Comput. Phys. (accepted for publication).

8. J. D. Ramshaw, P. J. O'Rourke, and A. A. Amsden, "Acoustic Damping for Explicit Calculations of Fluid Flow at Low Mach Number," manuscript in preparation.

9. J. K. Dukowicz, J. Comput. Phys. 35, 229 (1980).

10. P. J. O'Rourke and F. V. Bracco, "Modelling of Drop Interactions in Thick Sprays and a Comparison with Experiments," Institution of Mechanical Engineers Paper C404/80, London (1980).

11. J. D. Ramshaw and A. A. Amsden, "Improved Iteration Scheme for Partial Equilibrium Flow," J. Comput. Phys. (accepted for publication).

12. A. Brandt, J. E. Dendy, and H. Ruppel, J. Comput. Phys. 34, 348 (1980).

13. P. J. O'Rourke, "The Acoustic Mode in Numerical Calculations of Subsonic Combustion," Workshop on Combustion, Flames, and Fires, Les Houches, France (1984).

14. F. H. Harlow and J. E. Welch, Phys. Fluids 8, 2182 (1965).

15. A. Barba, et al., Comp. Meth. in Appl. Mech and Eng., 44, 49 (1984).

16. P. J. O'Rourke, "Collective Drop Effects on Vaporizing Liquid Sprays," Princeton University thesis 1532-T (1981).

17. J. O. Hirschfelder, C. F. Curtiss, and R. B. Bird, Molecular Theory of Gases and Liquids, John Wiley and Sons, New York (1954).

18. M. Neiburger, et al., "The Role of Drop Dynamics in the Physics of Clouds and Rain," Intern. Colloq. on Drops and Bubbles, Cal. Inst. of Tech. and Jet Propulsion Laboratory (1974).

19. P. R. Brazier-Smith, S. G. Jennings, and J. Latham, Proc. R. Soc. Lond. A, 326, 393 (1972).

20. L. Martinelli, R. D. Reitz, and F. V. Bracco, "Comparisons of Computed and Measured Dense Spray Jets," 9th Int. Coll. on Dyn. of Expl. and Reactive Systems, Poitiers, France (1983).

21. A. U. Chatwani and F. V. Bracco, "Computation of Dense Spray Jets," Intern. Conf. on Liquid Atomization and Spray Systems (1985).